JOURNAL OF BACTERIOLOGY, Feb. 1991, p. 1268–1278
0021-9193/91/031268-11$02.00/0

Vol. 173, No. 3

Mutations in the *Escherichia coli dnaG* Gene Suggest Coupling between DNA Replication and Chromosome Partitioning

MARKUS GROMPE,[1] JAMES VERSALOVIC,[1] THEARITH KOEUTH,[1] AND JAMES R. LUPSKI[1,2]*

Institute for Molecular Genetics[1] and Department of Pediatrics,[2] Baylor College of Medicine, One Baylor Plaza, Houston, Texas 77030

Received 31 August 1990/Accepted 27 November 1990

Eleven conditional lethal *dnaG*(Ts) mutations were located by chemical cleavage of heteroduplexes formed between polymerase chain reaction-amplified DNAs from wild-type and mutant *dnaG* genes. This entailed end labeling one DNA strand of the heteroduplex, chemically modifying the strands with hydroxylamine or osmium tetroxide (OsO_4) at the site of mismatch, and cleaving them with piperidine. The cleavage products were electrophoresed, and the size corresponded to the position of the mutation with respect to the labeled primer. Exact base pair changes were then determined by DNA sequence analysis. The *dnaG3*, *dnaG308*, and *dnaG399* mutations map within 135 nucleotides of one another near the middle of *dnaG*. The "parB" allele of *dnaG* is 36 bp from the 3′ end of *dnaG* and 9 bp downstream of *dnaG2903*; both appear to result in abnormal chromosome partitioning and diffuse nucleoid staining. A suppressor of the *dnaG2903* allele (*sdgA5*) maps within the terminator T_1 just 5′ to the *dnaG* gene. Isogenic strains that carried *dnaG2903* and did or did not carry the *sdgA5* suppressor were analyzed by a combination of phase-contrast and fluorescence microscopy with 4′,6-diamidino-2-phenylindole to stain DNA and visualize the partitioning chromosome. Overexpression of the mutant *dnaG* allele corrected the abnormal diffuse-nucleoid-staining phenotype associated with normally expressed *dnaG2903*. The mutations within the *dnaG* gene appear to cluster into two regions which may represent distinct functional domains within the primase protein.

The *dnaG* gene product, primase, synthesizes a primer RNA to initiate DNA replication (3, 4, 42, 43). In an in vitro phage G4 DNA replication system, primase has been shown to interact with the replication origin (G4ori_c), producing primer RNA prior to DNA synthesis (15, 17). A 5′-CTG-3′ trinucleotide flanking stem loop I that serves as the complement for the start of the newly synthesized primer appears to be essential in signaling the initiation of primer synthesis (15, 16). The *dnaG* gene product is required to initiate DNA synthesis at the *Escherichia coli* chromosomal origin (*oriC*) of DNA replication (47) and for the priming of Okazaki fragment lagging-strand synthesis (25).

The *dnaG* gene is 1,746 nucleotides (582 codons) long, and several regulatory sites are adjacent to or within the gene (6, 27, 28, 30, 31, 38, 46). A terminator structure (T_1) is just upstream of the *dnaG* start codon, and transcription of the gene seems to be regulated by antitermination (1, 29, 31, 46, 51). There are three promoters just before the 3′ end of *dnaG*, and in addition there is an RNA-processing site immediately adjacent to its translation termination codon (6).

The existence of the mutations in *dnaG* with conditional lethal (temperature-sensitive) phenotypes demonstrates that primase protein is essential for cell growth. Both missense temperature-sensitive mutants and amber mutations, in a *supF*(Ts) background, have been described. Phenotypes associated with specific *dnaG*(Ts) mutations include "quick-stop" mutants, in which DNA synthesis immediately stops at 42°C (*dnaG308* and *dna399*), and "slow-stop" mutants (*dnaG3*, *dnaP*, or *dnaG2903*), in which residual synthesis occurs at restrictive 42°C. Quick-stop mutations probably affect elongation of the replication fork, while slow-stop mutations might affect the initiation of chromosomal DNA replication. Recently, the *parB* mutation has been found to be a *dnaG* allele and to confer a partial defect in both initiation and elongation of DNA replication at nonpermissive temperatures (39).

The *parB* (39) mutant is one of the *par* strains identified by Hirota et al. (19) which continue synthesizing DNA but keep the chromosomes centrally located rather than partitioned along filaments. The *dnaP* allele was originally isolated by screening temperature-sensitive strains for phenethyl alcohol resistance, which has been interpreted to suggest an interaction between the replication apparatus and the membrane (48). It is a *dnaG* allele, *dnaG2903* (36), and has morphologic characteristics indicative of deficient chromosome partitioning, such as an abnormal nucleoid structure (48). In *dnaP* cells, altered cell membrane properties have been reported, indicating a possible interaction of primase with the cell membrane (48). Several suppressor mutants of *dnaG2903* have been isolated, and two of these (*sdgA5* and *sdgA6* [21]) are due to point mutations in T_1, the terminator that precedes the *dnaG* gene. Transcription of *dnaG* is increased in these mutants because of deficient termination, and the overproduction of the altered *dnaG2903* gene product suppresses the growth defect (21). The exact role of the primase protein in the chromosome separation process is not known, and it is therefore unclear whether these defects in partitioning represent a secondary effect of impaired DNA replication or possibly a separate function of the *dnaG* protein. Determining the exact location of the different mutations in the *dnaG* gene may help clarify the functional roles of DnaG.

In this paper we report the analysis of 11 *E. coli* strains which are conditional lethal for growth with mutations that map to the *dnaG* locus. The site of the mutations within the *dnaG* gene was determined by chemical mismatch cleavage (8–11, 13), and the actual base pair change was determined by DNA sequencing. The mutations map to two regions

* Corresponding author.

TABLE 1. Bacterial strains

Strain	Description	Source or reference
PC3	F⁻ *dnaG3 leuB6 thyA47 rpsL153 deoC3* λ⁻	B. Bachmann (7, 50)
CR34/308	F⁻ *dnaG308 thr-1 leuB6 thyA6 thi-1 deoC1 lacY1 strA67 tonA21 supE44* λ⁻	B. Bachmann (14, 33)
CR34/399	F⁻ *dnaG399 rpoD800 thr-1 leuB6 fhuA21 lacY1 supE44 rfbD1 thyA6 rpsL67 thi-1 deoC1* λ⁻	B. Bachmann (14, 33)
KY1420	*dnaG9*(Am) *ilv thr metE trpE9829*(Am) *tyr*(Am) *thy supF*(Ts6)	Y. Nakamura (37)
KY1421	*dnaG24*(Am) *ilv thr metE trpE9829*(Am) *tyr*(Am) *thy supF*(Ts6)	Y. Nakamura (37)
KY 1422	*dnaG26*(Am) *ilv thr metE trpE9829*(Am) *tyr*(Am) *thy supF*(Ts6)	Y. Nakamura (37)
GC2530	*parB thr-1 leu-6 proA2 his-4 argE3 thi-1 lacY1 galK2 ara-14 xyl-5 mtl-1 tsx-33 sup-37 rpsL31*	R. D'Ari (19, 39)
KY2750	*dnaP thr-1 leuB6 trp-67 his-100 met-99 thi-1 ara-13 lacY1 gal-6 xyl-7 mtl-2 malA1 azi-8 rpsL135* (=*strA135*) *tonA2 supE44*	B. Bachmann (36, 48)
W3110	Prototroph	T. Katayama (36)
KN1378	*dnaG2903* in W3110 background	T. Katayama (21, 36)
KA5	*sdgA5* in W3110 background	T. Katayama (21)
KA6	*sdgA6* in W3110 background	T. Katayama (21)
HB101	F⁻ *hsdS20* r_B^- m_B^- *recA13 ara-14 proA2 lacY1 galK2 rpsL20* Sm^r *xyl-5 mtl-1 supE44* λ⁻	5

within the *dnaG* gene which may correspond to or encode different functional domains of DnaG.

MATERIALS AND METHODS

Bacterial strains. The bacterial strains used were derivatives of *E. coli* K-12 and are listed in Table 1 (2, 7, 14, 21, 33, 36, 37, 39, 48, 50). Strains HB101 (5) and W3110 (21) were used as wild-type *dnaG* controls.

Polymerase chain reaction (PCR). Genomic DNA (0.5 μg) was isolated from each strain by standard procedures (32) and was amplified for 30 cycles, with primers B and D for the 5′ region of the *dnaG* gene and primers C and F for the 3′ end (see Fig. 2). The primer sequences were as follows: B, 5′-GAATTGCTAAAAATCGGGGCCT-3′; D, 5′-CTAGCG TGTCAGGGTCTTCGCC-3′; C, 5′-GTTCCGCGCGACCA ACAATGTC-3′; and F, 5′-GCCAACGATAATTACGAGG GCG-3′. Additional primers α (5′-CGCAGGAAGTTTCAA TACCC-3′) and β (5′-CACGCGTGGAAATTCTTGCC-3′) were used to analyze the *dnaG* upstream regulatory region. *Taq* polymerase (Cetus) (5 U) was used in each amplification, and the buffer, deoxyribonucleotide concentration, and primer concentration were as described by Kogan et al. (24). The reaction mixture volume was 100 μl. Amplification conditions were as follows. An initial denaturation step of 7 min at 94°C was followed by 30 cycles of 90°C for 30 s, annealing at 60°C for 1 min, and polymerase extension at 72°C for 3 min. After this, a final extension step of 72°C for 6 min was added. Five microliters of each amplification reaction mixture was electrophoresed in a 1% agarose gel and stained with ethidium bromide to estimate the quantity and verify the size of the amplification product.

The products were purified with a Centricon 100 column (Amicon) and frozen at a concentration of 1 ng/μl. Products were 5′ end labeled as follows: 3.5 pmol of primer (~30 ng), 10 μl of γ[^{32}P]ATP (6,000 Ci/mmol, 10 μCi/μl), 3 μl of 10× kinase buffer (Tris hydrochloride [0.5 M, pH 7.6], $MgCl_2$ [0.1 M], dithiothreitol [0.15 M]) was mixed, and H_2O was added to a volume of 30 μl. T4 polynucleotide kinase (10 U) was added, and the mixture was incubated at 37°C for 45 min. The γ[^{32}P]ATP-to-end ratio was approximately 5:1. The reaction mixture volume was then brought up to 1 ml, and the labeled oligonucleotide was purified and concentrated to 40 μl by centrifugation through a Centricon 3 (Amicon) column. One nanogram of each wild-type PCR stock was then reamplified in four separate reactions employing one labeled and the corresponding unlabeled primer. The reamplifications resulted in the strand-specific radiolabeled PCR probes B*D, BD*, C*F, and CF*, with the asterisks indicating the labeled primer. The amplification conditions, except for the reaction mixture volume and the primer concentrations, were identical to the ones used for the PCR from genomic DNA.

Chemical cleavage of mismatched bases: preparation of heteroduplexes. The chemical mismatch cleavage procedure was performed on DNA heteroduplexes consisting of a radiolabeled wild-type strand and an unlabeled mutant strand. PCR products from strain W3110 served as templates for preparing radioactive wild-type probes. First, stocks of wild-type PCR products BD and CF from the 5′ and the 3′ regions of the gene, respectively, were made. A second set of amplifications with one radiolabeled primer and employing these stocks was performed. Each of the four primers (B, D, C, and F) was labeled separately. Approximately 3 pmol (80%) of the labeled primer was used with an equal amount of the corresponding unlabeled primer in a total reaction volume of 60 μl. After amplification, the probes were purified in a 1% low-melting-point agarose gel, extracted by electroelution into a Centricon 100 (Amicon) column according to manufacturer's instructions, and adjusted to ~10 ng/μl (~50,000 cpm). PCR was also carried out on mutant-strain genomic DNA, and the reaction products were purified by centrifugation through a Centricon 100 column. After quantitation the DNA was stored frozen at a concentration of 50 ng/μl.

Unlabeled target (mutant PCR product) (150 ng) and 10 ng of the wild-type labeled probe were mixed in 6 μl of 5× annealing buffer (3 M NaCl, 30 mM Tris hydrochloride buffer, pH 7.7, 35 mM $MgCl_2$), and the volume was adjusted to 30 μl. The mixture was then heated in a 1.5-ml tube in a boiling water bath for 5 min. The droplets were pooled by centrifugation, and the tubes were transferred to a 42°C water bath for 2 h. Ice-cold ethanol (90 μl) was added, and the mixture of heteroduplex and single-strand DNA was precipitated.

Mismatch-specific chemical modification of heteroduplex DNA and piperidine cleavage. Mismatched bases, resulting from the heteroduplex formed between mutant and wild-type sequences, are susceptible to chemical modification, and the modified bases are susceptible to piperidine cleavage as originally developed by Cotton et al. (10). One detailed method, evolved from theirs, is as follows. The precipitated heteroduplex DNA was redissolved in 20 μl of H_2O, and 6 μl

of this was used for the subsequent chemical-modification reactions which were carried out in siliconized 1.5-ml tubes. For the hydroxylamine reaction, 20 μl of hydroxylamine solution (1.39 g of hydroxylamine chloride in 1.6 ml of H_2O, buffered to pH 6.0 with diethylamine) was mixed with the heteroduplex and then incubated at 37°C for 20 min. In the osmium tetroxide reaction, 2.5 μl of 10× osmium buffer (100 mM Tris hydrochloride, pH 7.7, 10 mM EDTA, 15% pyridine) was first added to each heteroduplex. The tubes were then placed on ice, and 15 μl of 2% osmium tetroxide (aqueous solution; Aldrich) was mixed thoroughly by pipetting up and down and incubated at 37°C for 5 min. Both the osmium tetroxide and the hydroxylamine reactions were stopped by the addition of 200 μl of stop buffer (0.3 M sodium acetate, pH 5.2, 0.5 mM EDTA, 25 μg of bakers' yeast tRNA per ml). The reaction mixture was precipitated with 750 μl of ethanol, washed once with 75% (vol/vol) ethanol–water, and dried.

The dried pellet was suspended in 50 μl of 1 M piperidine and incubated at 90°C for 30 min. An equal volume of 0.6 M sodium acetate, pH 5.2, and 300 μl of ethanol were added for precipitation. After a final wash with 75% (vol/vol) ethanol–water, the reaction mixtures were dried and redissolved in 15 μl of formamide loading buffer. Then 3 to 6 μl was electrophoresed in a 4% wedged denaturing polyacrylamide gel. The gels were fixed with methanol-acetic acid-water (1:1:8), dried, and exposed to Kodak X-ray film for 24 h.

DNA sequence analysis. Agarose gel-purified PCR products (see above) were kinased as described above, but with unlabeled ATP at a final concentration of 1 mM. The DNA was extracted with phenol and chloroform; ethanol precipitated (32); ligated into *Sma*I-cut, calf intestinal phosphatase-treated vector pTZ19R (35), and transformed into strain XL1-Blue (Stratagene). A single-strand DNA template was prepared by coinfection with helper M13 phage according to standard procedures (32), and dideoxy-chain termination sequencing was performed as described by Sanger et al. (44), with the oligoprimer closest to the mutation site detected by chemical mismatch cleavage as a sequencing primer.

Combination fluorescence-phase-contrast microscopy. Cells were grown for 12 to 14 h at 32°C in Luria-Bertani (LB) broth (32) supplemented with 0.01% thiamine. They were then diluted 1:20 and grown for 2 to 3 h to log phase (optical density at 600 nm, 0.6 to 0.8) at 32 or 42°C in LB supplemented with 0.36% glucose and 0.01% thiamine.

Cell replication was temporarily arrested by inhibiting protein synthesis, since optimal photomicrographs showing uniformly sized cells were obtained starting with synchronized cells. To synchronize growth, a 1:10 dilution of cells was grown in either LB supplemented with 20 μg of chloramphenicol per ml or M9 minimal medium (with 0.2% glucose) and incubated for 2 to 3 h at 32 or 42°C. After synchronization, cells were collected, suspended in 0.84% NaCl, and washed three times to eliminate the chloramphenicol. The washed cells were resuspended in LB with 0.36% glucose and 0.01% thiamine and incubated at 32 or 42°C for 3 h. Collected samples were washed in 0.84% NaCl, resuspended in 10 μl of 0.84% NaCl, and added to a glass slide.

The slides were air dried at room temperature and fixed with methanol. After rinsing with tap water, 10 μl of poly-L-lysine (Sigma) solution (5 μg/ml) was added and the slides were dried at room temperature. Then 10 μl of 4′,6-diamidino-2-phenylindole (Boehringer Mannheim) solution (5 μg/ml) was added to the dried slide, and a coverslip was added. The stained cells and nucleoids were visualized with a Zeiss Axiophot Microscope, ×2,000 magnification, by the "fluo-phase" method (18). Photographs were taken with Ektachrome 400 film.

Phenethyl alcohol resistance. Overnight cultures were diluted 1:10 and grown to log phase (optical density at 600 nm, 0.6 to 0.8) at 32°C. The log-phase cells were serially diluted in 0.84% NaCl and plated on LB supplemented with 0.15% *R*-(+)-*sec*-phenylethyl alcohol (Sigma) to obtain 10^2 to 10^3 CFU/100-mm plate. Plates were incubated at 32°C for 14 h. Colonies were counted and compared with the same strain at the same dilution on LB alone as a control. The percent colony survival was then tabulated.

RESULTS

Thermosensitive growth phenotype of *dnaG* mutant strains. Temperature sensitivity was confirmed and most pronounced with the *dnaG3* and *dnaG399* alleles, as demonstrated by the lack of growth at 37°C (Fig. 1). As expected, none of the *dnaG*(Ts) strains grew normally at 42°C. Of the *dnaG*(Am) mutants in a *supF*(Ts) background, the *dnaG26*(Am) strain gave the smallest colonies and appeared to grow the most poorly at permissive 32°C.

Although *dnaP* and *dnaG2903* are the same *dnaG* allele (see below), they were harbored in different strain backgrounds. The *dnaG2903* strain used here was constructed by placing the *dnaG* allele on a wild-type (W3110) background (21), while *dnaP* is from the original mutant strain (36, 48). Given the fact that there was partial growth at 42°C with *dnaP*, it is likely that this strain contains additional mutations in genes other than *dnaG* that modify the phenotype. At 43 to 44°C the *dnaP* strain did not grow. The fact that the *dnaG2903* allele when placed in the wild-type prototrophic strain W3110 background still displayed a conditional lethal phenotype suggest that this phenotype results from a mutation at the *dnaG* locus. Suppression of the temperature-sensitive phenotype of the *dnaG2903* allele by the *sdgA* suppressors was verified by demonstrating normal growth at 42°C.

Analysis of mutations. The sites of mutation in *dnaG* were determined by the chemical mismatch cleavage method with 1-kb PCR products amplified in two separate reactions: BD and CF (Fig. 2). None of the PCR products from mutants differed in size from the wild type, thus ruling out any major deletions or insertions (data not shown). Both an osmium tetroxide reaction, which chemically modifies mismatched thymidines, and a hydroxylamine reaction, which modifies mismatched cytosine residues, were performed for each of the four strand-specific PCR probes (B*D, BD*, C*F, and CF*), thereby ensuring that all possible changes would be detected. One, and sometimes more than one, chemical-cleavage reaction product was found for each *dnaG* mutant strain. Only the regions in which a mutation was detected by cleavage were then analyzed by dideoxy sequencing. A total of 2,300 bp was sequenced, after cloning PCR products from 11 strains, and the only base alterations found were those detected by chemical mismatch cleavage. This indicates a frequency of errors introduced by *Taq* polymerase (41) of less than 1 in 2,300 of the clones sequenced. The *dnaG* wild-type sequence published by Burton et al. (6) was used as a reference. In that paper, several differences from the originally published (46) *dnaG* sequence were noted. In all cases our sequence data agreed with those of Burton et al. (6), thus confirming the corrections of the original DNA sequence. The detected sequence alterations resulting in *dnaG* mutant alleles are summarized in Table 2 and are described in detail below.

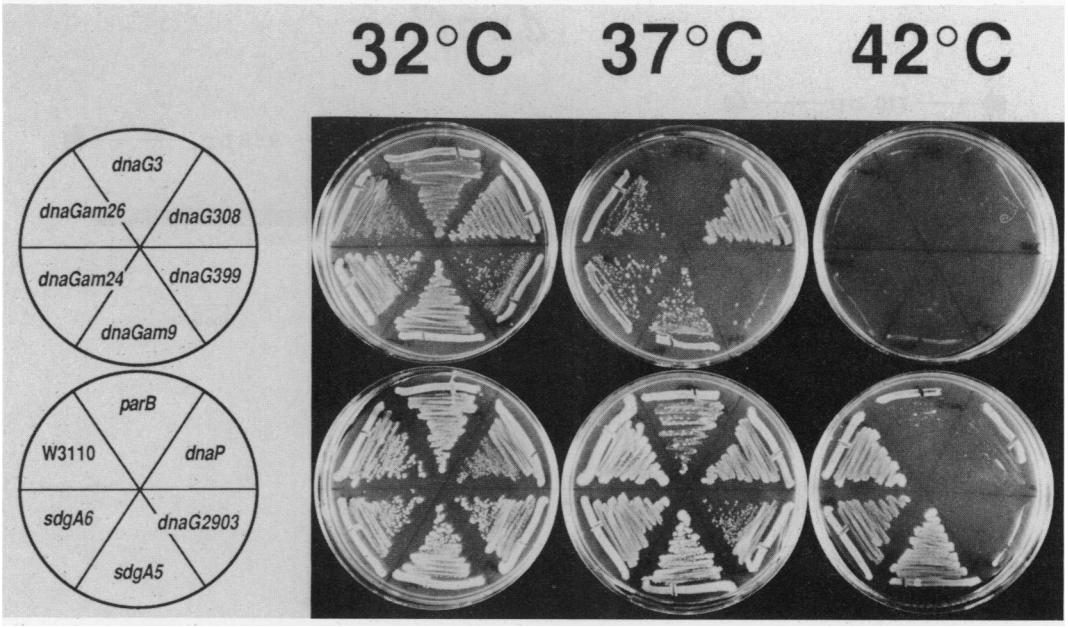

FIG. 1. Temperature sensitivity of *dnaG* allelic strains. Plates were prepared as described in Materials and Methods. Wild-type control W3110 and suppressors of the *dnaG2903* alleles, *sdgA5* and *sdgA6*, were resistant to high temperatures, as evidenced by growth at 42°C. All of the *dnaG* allele-containing strains were temperature sensitive and did not grow at 42°C. Note that strains harboring the *dnaG3* allele or *dnaG399* allele display extreme temperature sensitivity, as evidenced by an absence of growth at 37°C. In this paper, these alleles are shown to be the same base pair change at the *dnaG* locus.

Amber mutations in *dnaG*. *dnaG* amber mutations, demonstrating temperature-sensitive phenotypes with a *supF*(Ts) background, were studied first, since they provided a control for the methodology: each should result from a mutation to TAG amber in-frame termination codons. This expectation was verified with each of the three cases analyzed. An example of the complete cleavage that locates the base pair change in the *dnaG24*(Am) allele is shown in Fig. 3. Cleavage bands were seen only in regions of true mismatches. A cleavage band (115 bp) was obtained only with probe B*D and hydroxylamine, indicating an unpaired cytosine at a mismatch 115 bp from the 5′ end of the primer B wild-type DNA or nucleotide 94 of the *dnaG* open reading frame. We can deduce that C (wild type) is mismatched with T (mutant not labeled), leading to a TAG stop codon, and this was tested rigorously by sequencing (see below). No other mismatch mutations were detected, which is in agreement with the results of the marker rescue experiments showing that *dnaG24*(Am) was between the *Hin*dIII site just 5′ to the *dnaG* AUG and the *Xho*I site at nucleotide 240 (37). The 5′ location of this mutation is polar on *rpoD* when *supF*(Ts) is thermally inactivated (37). The mutation detected by chemical mismatch cleavage at nucleotide 94 therefore fulfilled predictions for both the expected sequence alteration and the position. Sequence analysis demonstrated the expected C-to-T transition at nucleotide 94. Closer examination of the cleavage product of *dnaG24*(Am) revealed a doublet (Fig. 4) as also found by Cotton and Campbell (9), who showed that base mismatching in heteroduplexes may destabilize contiguous base pairs and thus may lead to several bands clustering around the true mutation site.

Conceivably, the three bands seen with *dnaG9*(Am) (Fig. 4) might have represented heteroduplex destabilization, although such destabilization is normally seen over a few base pairs and these three bands extend over approximately 10 bp, but DNA sequencing demonstrated that each band represented a unique guanosine (G)-to-adenosine (A) mismatch. The sequence analysis of the mismatched region is shown in Fig. 5a. Only one of the transitions (nucleotide 1565) leads to an amber codon. The change in nucleotide 1557 is conservative, and the mutation at nucleotide 1549 changes glutamic acid to lysine in the protein. This result illustrates an important feature of the chemical-cleavage methodology. It can detect multiple clustered sequence alterations in the same strand, since the conditions were chosen to give incomplete cleavage. The shortest cleavage product gave the strongest signal, but the other two remained clearly detectable (Fig. 4). The mismatch in *dnaG26*(Am) was found by using probe C*F and hydroxylamine, indicating a cytosine alteration and confirmed by DNA sequencing.

Mutants thermosensitive for DNA synthesis cluster in two regions of the *dnaG* structural gene. Chemical cleavage analysis was performed on the 11 mutant strains shown in Table 1 by scanning the *dnaG* structural gene to detect the position of the mutation. For each *dnaG* strain, all eight chemical-cleavage reactions were performed as in the analysis of *dnaG24*(Am). The results (Fig. 4) are shown only for the individual chemical-cleavage reactions in which a cleavage product was detected. Two separate cleavage products were seen in *dnaG308*, one with probe BD* and osmium tetroxide and one with B*D and hydroxylamine. The first was due to an A-to-T transversion at nucleotide 755, changing glutamine 252 to leucine, and the second was due to a C-to-T transversion at nucleotide 620, altering proline 207 to leucine. Both changes represent nonconservative changes and are of potential functional significance. Glutamine is polar, leucine is a hydrophobic amino acid, and proline

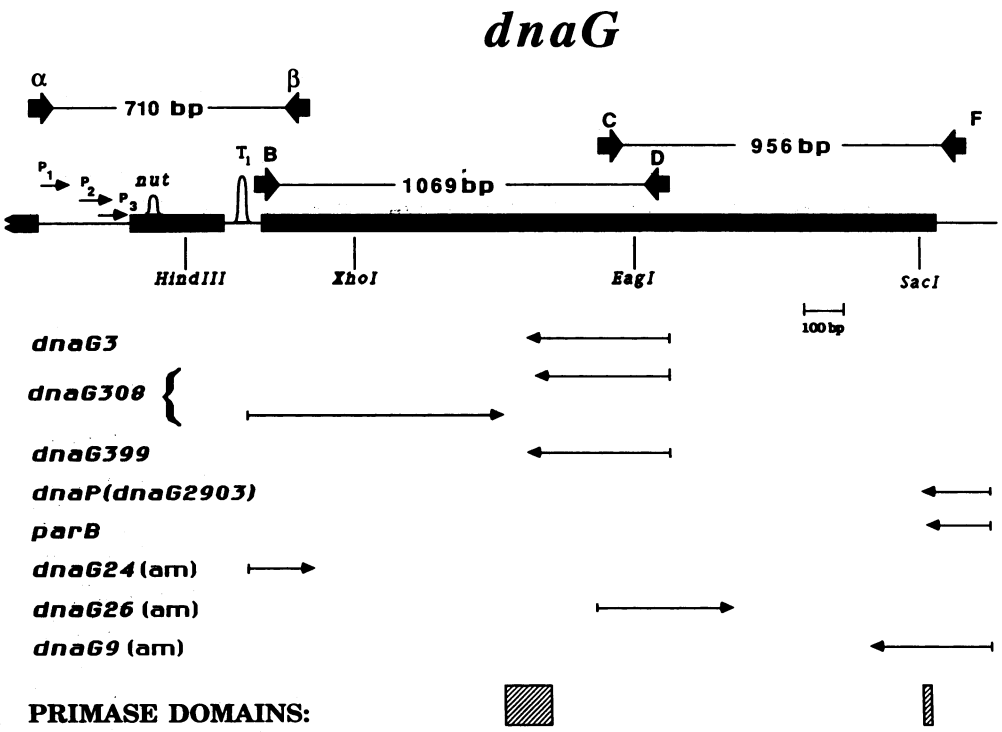

FIG. 2. *dnaG* gene structure and PCR primers. The *dnaG* gene with its regulatory elements and important restriction sites is shown in the top half of the figure. P_1, P_2, P_3, Promoter elements; T_1, terminator structure; *nut*, nut_{eq} site (28, 29, 31). The positions of PCR primers B, C, D, and F are marked by fat arrows, and the lengths of the respective PCR products are given. In the lower half of the figure, cleavage products obtained from the different *dnaG* mutant strains are indicated by arrows. The tip of each arrow marks the location of the mutation. The bar at the beginning of each arrow corresponds to the radiolabeled PCR primer used in the mutation detection. The lengths of the arrows correspond to the cleavage products in Fig. 3 and 4. At the bottom of the figure, the regions in which the conditional lethal *dnaG* mutations were located, corresponding to candidate DnaG domains, are indicated by striped bars.

results in sharp bends in polypeptide chains which affect protein tertiary structure.

dnaG3 and *dnaG399* resulted in identical cleavage products, a 300-bp fragment from BD* after hydroxylamine treatment, and sequence analysis showed that each mutation was due to a G-to-A transition at nucleotide 740 (codon 247). Since these alleles were isolated in different laboratories and strain backgrounds and had different phenotypes (*dnaG3*, residual DNA synthesis; *dnaG399*, quick stop), we tested for a possible strain mix-up by again obtaining these strains from the *E. coli* Genetic Stock Center. The G-to-A mutation creates a *Sau*3A restriction site, and this new site was found with the PCR-amplified chromosomal DNA from each of these mutant strains (data not shown). No additional cleavage products were detected in either mutant by either chemical cleavage or DNA sequencing, indicating that a second site alteration in *dnaG* does not explain the different phenotypes. It is known that strain CR34/399 harbors an additional mutation in the gene encoding the sigma subunit of RNA polymerase, *rpoD* (*rpoD800*) (26), and this or other unknown mutations probably contribute to its altered phenotype.

Previously, it was demonstrated that *dnaP* is a *dnaG* allele (*dnaG2903*) and extragenic suppressors of *dnaG2903*, *sdgA5* and *sdgA6*, are point mutations in T_1. By our analysis, strains harboring *dnaP* (*dnaG2903*) and suppressors *sdgA5* and *sdgA6* were found to contain the original *dnaG* mutation as expected by hydroxylamine modification and cleavage of the CF* probe. The sequence alteration responsible in these strains is a G-to-A transition in nucleotide 1699, changing glutamic acid 567 to lysine (Fig. 5b and Table 2). The possibility of additional mutations occurring in the *sdgA* strains was examined by scanning the regions upstream of *dnaG* by using primers α and β (Fig. 2). Only one cleavage product whose size corresponded to a base pair change in T_1 (21) was found (data not shown). The suppression of the temperature-sensitive phenotype of *dnaG2903* in *sdgA5* and *sdgA6* strains therefore is most likely attributable to the mutations in the terminator structure.

parB resembles *dnaG2903* in phenotype (39), and the *parB* mutation maps 9 bp downstream at nucleotide 1708. The mutation leads to a glutamic acid (570)-to-lysine change in DnaG. Figure 5b shows the sequence analysis of this region for both strains. The mutation in *parB* obliterates a *Sac*I restriction site, and this was confirmed by restriction digestion of PCR-generated CF fragments with chromosomal DNA from *parB*, *dnaG2903*, and W3110 strains (data not shown).

Phenotypic characterization of strains harboring *dnaG* alleles. To examine the phenotype resulting from specific mutations at the *dnaG* locus, isogenic strains harboring *dnaG2903* and its suppressors (*sdgA5* and *sdgA6*) were examined by combination fluorescence-phase-contrast microscopy with W3110 as the isogenic wild-type control. The combined fluo-phase method (18) was used for photography to illustrate nucleoid shape and cellular morphology simultaneously. The nucleoid shape was independent of the method of synchronization (by chloramphenicol or M9 minimal medium).

W3110 exhibited the characteristic rod shape of *E. coli*

TABLE 2. Mutations at the *dnaG* locus

dnaG allele	Mutagen[a]	Phenotype[b]	Mutation(s)
dnaG3	NTG	Residual DNA synthesis at 42°C (initiation mutant)	Codon 247 (GGT→GAT, Gly→Asp)
dnaG308	NTG	Immediate stop of DNA synthesis at 42°C (elongation mutant)	Codon 252 (CAG→CTG, Gln→Leu) Codon 207 (CCC→CTC, Pro→Leu)
dnaG399	NTG	Immediate stop of DNA synthesis at 42°C (elongation mutant)	Codon 247 (GGT→GAT, Gly→Asp)
dnaG9(Am)	HA		Codon 517 (GAA→AAA, Glu→Lys) Codon 519 (CTG→CTA, Leu→Leu) Codon 522 (TGG→TAG, Trp→stop)
dnaG24(Am)	HA	Polar on *rpoD*	Codon 32 (CAG→TAG, Gln→stop)
dnaG26(Am)	HA		Codon 413 (CAG→TAG, Gln→stop)
parB	NTG	Chromosome partition mutant; continues to synthesize DNA but keeps the chromosomes centrally located rather than partitioned along the filaments, DNA replication perturbed in both initiation and elongation; abnormal nucleoid structure	Codon 570 (GAG→AAG, Glu→Lys)
dnaP (*dnaG2903*)[c]	NTG	Residual synthesis at 42°C; alteration in membrane structure affects sensitivity to phenylethyl alcohol, sodium deoxycholate, and rifampin; abnormal nucleoid structure.	Codon 567 (GAA→AAA, Glu→Lys)
dnaG2903	NTG	Same as *dnaP*	Codon 567 (GAA→AAA, Glu→Lys)
dnaG2903, *sdgA5*		Grows at 42°C	Codon 567 (GAA→AAA, Glu→Lys, nucleotide −43 in T_1 (G→A)
dnaG2903, *sdgA6*		Grows at 42°C	Codon 567 (GAA→AAA, Glu→Lys), nucleotide −62 in T_1 (C→A)

[a] NTG, *N*-Methyl-*N'*-nitro-*N*-nitrosoguanidine; HA, hydroxylamine.
[b] All of the *dnaG* alleles cause conditional lethal (temperature-sensitive) mutants which grow normally at 32°C but will not grow at 42°C.
[c] *dnaP* was renamed *dnaG2903* when it was found to be a *dnaG* allele (36).

with centrally located, discrete, round nucleoids (one to two per cell). The *dnaG2903* strain was wild type in morphology at 32°C but exhibited dramatic cell filamentation as seen with the other *dnaG* mutant strains at the restrictive temperature (Fig. 6). Strains harboring the *parB* mutation are indistinguishable from the *dnaG2903* strain with respect to cell and nucleoid morphology at the nonpermissive temperature of 42°C (data not shown). A diffuse nucleoid pattern had been reported in a *parB* strain studied by autoradiography (39), while a dispersed nucleoid structure had been observed for a *dnaP* (*dnaG2903*) strain studied by electron microscopy (48). The extragenic suppressor mutant for *dnaG2903*, *sdgA5*, exhibited wild-type cellular and nucleoid morphology at the restrictive temperature (Fig. 6), and *sdgA6* at a different site in the terminator exhibited an identical pattern (data not shown).

The *dnaP* strain was previously demonstrated to be relatively resistant to phenethyl alcohol. We examined resistance to phenethyl alcohol in strains in which the mutation in *dnaG* mapped to the carboxy terminus (*dnaG2903* and *parB*) and compared these results to the *dnaG* mutant strains that clustered in a different region (*dnaG308* and *dnaG399*). Although these are not isogenic strains, the fact that the temperature-sensitive growth phenotype in all strains is suppressed by either complementation or marker rescue with a recombinant plasmid containing the *dnaG* gene (pGL444 [30]) suggests that this phenotype results from mutations at the *dnaG* locus (data not shown). Strains harboring the *dnaG2903* allele were resistant, as demonstrated by the 95% colony survival on LB plates supplemented with 0.15% phenethyl alcohol compared with the 80% colony survival for wild-type W3110. Interestingly, a strain harboring the mutation mapping close to *dnaG2903*, the *parB* allele, behaved reproducibly in a very similar manner, with 75% colony survival on 0.15% phenethyl alcohol. Strains harboring the *dnaG308* or *dnaG399* allele were much more sensitive to phenethyl alcohol than wild-type W3110, with less than 1% of the colonies surviving. It is important to note that despite the differences in strain background, the precise location of the *dnaG* mutation clearly separates these strains with respect to phenethyl alcohol resistance.

DISCUSSION

We have used PCR amplification and specific cleavage at mismatched sites in heteroduplex DNAs to quickly locate interesting mutations in the *dnaG* gene. The *dnaG3*, *dnaG308*, and *dnaG399* mutations defective in DNA synthesis were located within 135 nucleotides of each other in the middle of the gene, whereas the *parB* and *dnaP* (*dnaG2903*) mutations defective in chromosome partitioning were in the last 50 nucleotides separated by 9 bp. *parB* and *dnaP* are the two *dnaG* alleles that suggest that the primase protein may be involved in chromosome partitioning. In *dnaP* strains, abnormal nucleoid organization and alterations in the membrane structure have been described, indicating that DnaG might interact with the cell membrane during division (48).

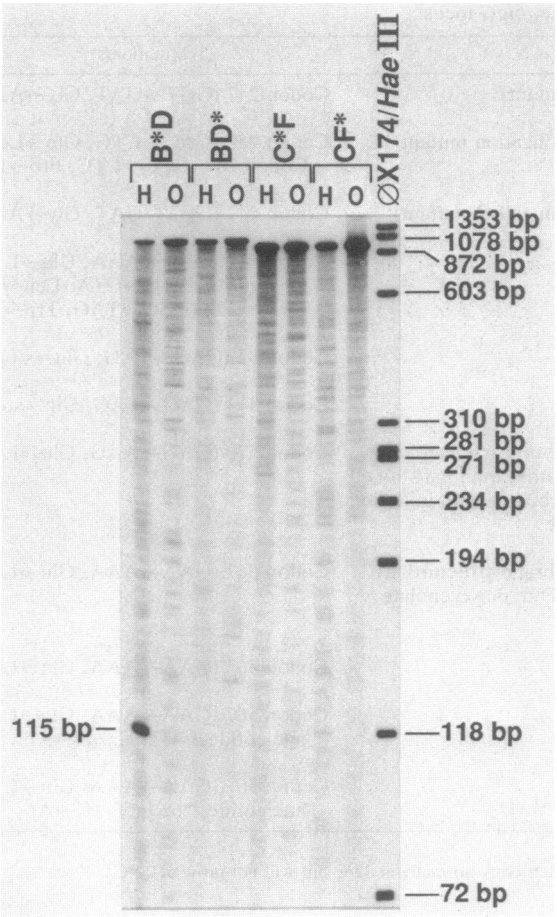

FIG. 3. *dnaG24*(Am) chemical mismatch cleavage gel. A complete chemical mismatch cleavage analysis for mutant *dnaG24*(Am) is shown. Eight reactions were performed, four with hydroxylamine (H) and four with osmium tetroxide (O). The four different PCR probes employed for the analysis are indicated at the top of the figure. The letters correspond to the primers used in the amplification; the radioactive primer is marked with an asterisk. A *Hae*III digest of ϕX174 was used as a size marker. The far left lane, in which hydroxylamine was used with probe B*D, shows positive cleavage at nucleotide 115 from the end of primer B. No cleavage was detected in any of the other lanes.

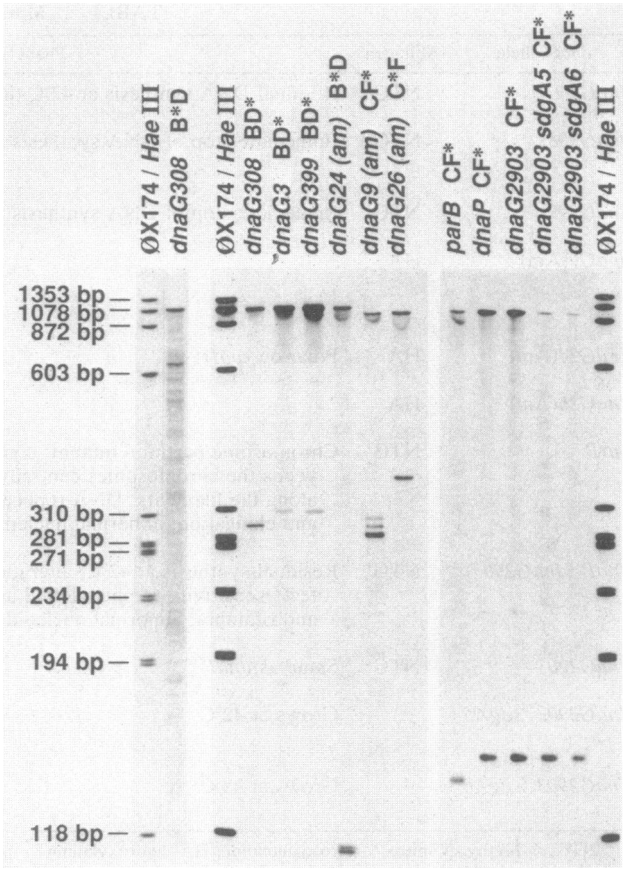

FIG. 4. Chemical mismatch cleavage summary gel: all chemical cleavage products obtained from the different *dnaG* mutant strains, with a *Hae*III digest of ϕX174 as a size marker. Above each lane the mutant strain as well as the radiolabeled PCR product used for detection is indicated. An asterisk marks the radioactive end of each probe (see also Fig. 2). Hydroxylamine was the modifying chemical in all lanes except *dnaG308* BD*, for which osmium tetroxide was used.

However, both of these mutant strains also show defects in DNA synthesis, so that it is not clear that the additional features indeed reflect primary functions of DnaG or represent secondary phenomena resulting from perturbed DNA replication.

Chemical cleavage analysis and DNA sequencing revealed three point mutations in the *dnaG9*(Am) strain. Only one generates an amber termination codon. The base pair change at nucleotide 1549 (codon 517) leads to a lysine substitution for glutamic acid. This alteration changes an acidic amino acid to a basic amino acid, yet colony formation is not affected, suggesting this position is not essential to primase function. The *dnaG26*(Am) mutation does not contain the most-5′ amber mutation, and yet a strain harboring this mutation grows most poorly on plates at 32°C (Fig. 1). The position of the TAG stop codon within the gene determines its context and thereby may influence suppression. Alternatively, insertion of a different amino acid during suppression alters primase structure and may affect function.

Amino acids 247 and 252 seem to be critical for primase function. In *dnaG399* and *dnaG3*, the amino acid change is from glycine 247 to aspartic acid, and in *dnaG308*, glutamine 252 is altered to leucine. Amino acids 247 and 252 are conserved in *Salmonella typhimurium* primase but are represented by asparagine and arginine in *Bacillus subtilis* primase. Neutral charge at position 247 and a polar amino acid at position 252 might therefore be important. Glutamic acid 570, which is altered to lysine in *parB*, resulting in a drastic change of charge, is conserved in different bacterial species. The degree of amino acid homology diverges in the carboxy termini from various species (12, 28, 49). Glutamic acid 567, the site affected by the *dnaG2903* mutation, is conserved in *S. typhimurium* but not in *B. subtilis*.

The mutations in *dnaG* occur in two regions that convey distinct phenotypic characteristics and may represent distinct functional domains in the DnaG protein. Strains harboring *dnaG3*, *dnaG308*, and *dnaG399* are sensitive to phenethyl alcohol, while strains with mutations at the 3′ end of *dnaG*, *parB* and *dnaG2903* strains, are relatively resistant to phenethyl alcohol and revert at a high frequency. Phenethyl alcohol is thought to exert a primary effect on the cell

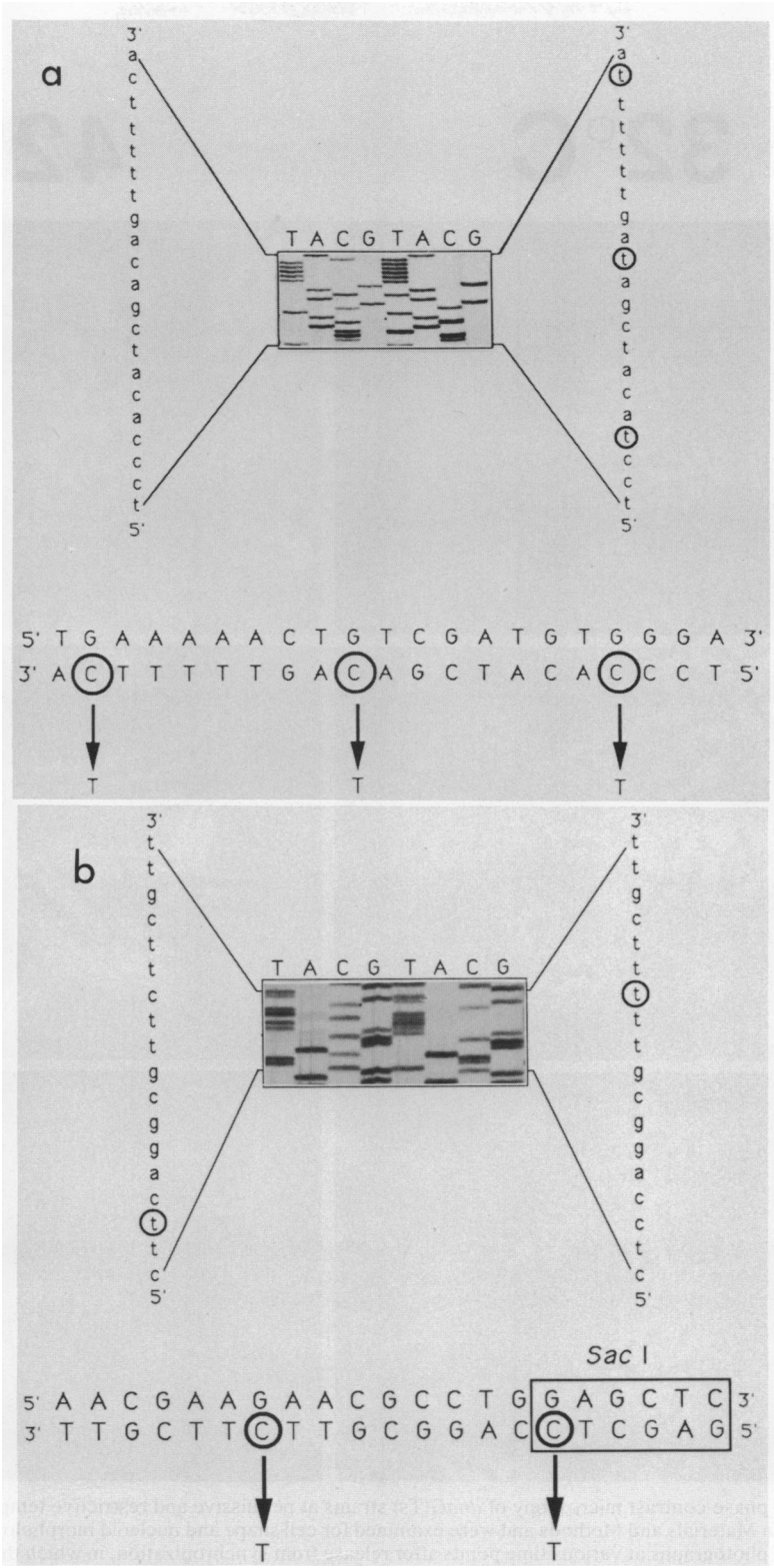

FIG. 5. DNA sequence analysis of wild-type *dnaG*, *dnaG9*(Am), *parB*, and *dnaG2903*. Autoradiograms of the DNA sequencing gels are shown with the actual DNA sequence readings to the left and right of the gels. Below the gels, the wild-type double-stranded *dnaG* sequence is given for this region. (a) DNA sequence analysis of mutant *dnaG9*(Am). On the left, a sequence ladder from a wild-type control is shown; on the right is the sequence in *dnaG9*(Am). Mutated bases are circled. (b) DNA sequence analysis of mutants *parB* and *dnaG2903*. On the left is the sequence of mutant *parB*, and on the right is that of *dnaG2903*. Altered bases are indicated by circles. The mutation in *parB* abolished a *Sac*I restriction site, indicated by a box.

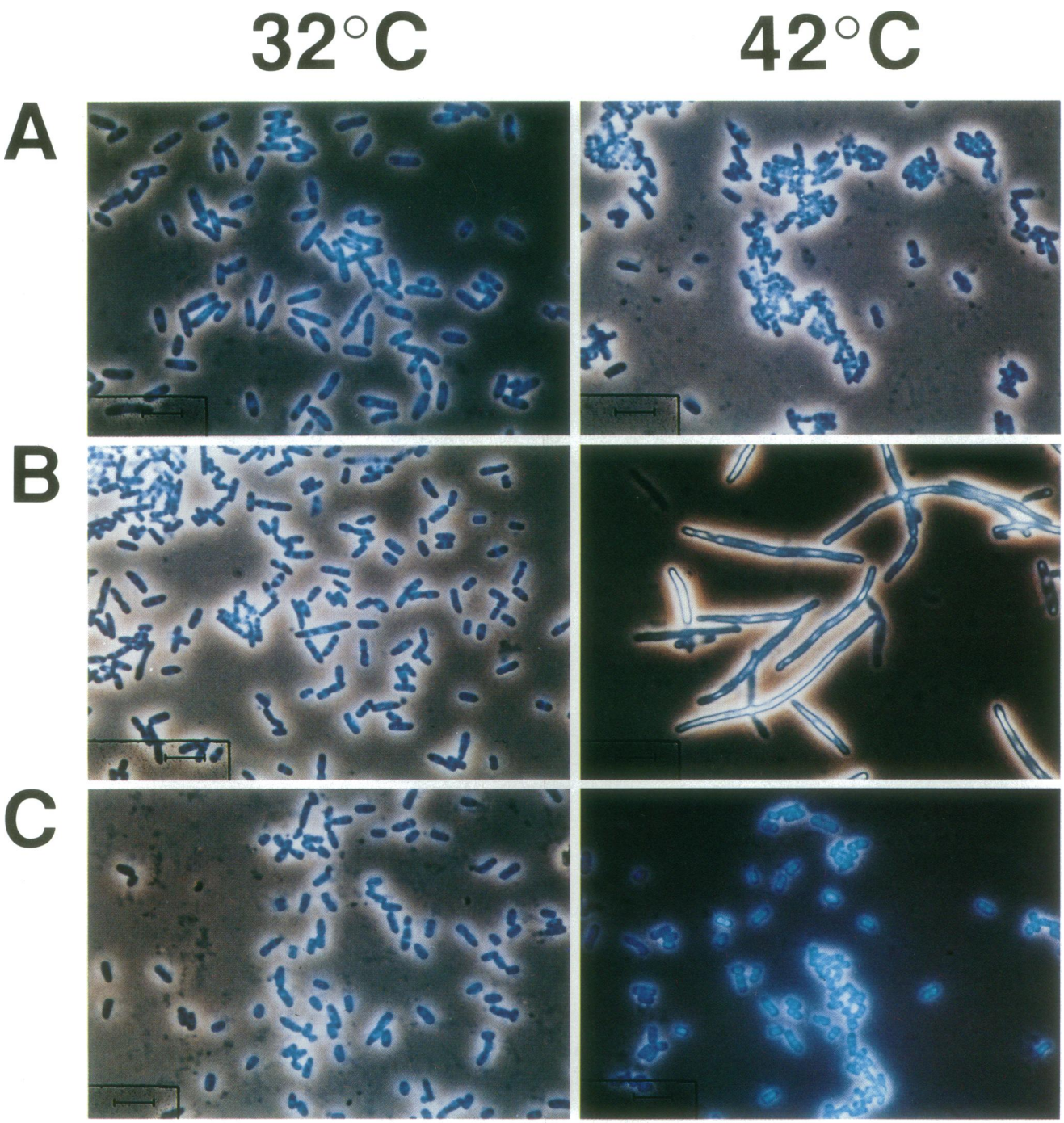

FIG. 6. Fluorescence and phase-contrast microscopy of *dnaG*(Ts) strains at permissive and restrictive temperatures. Cells were prepared for microscopy as described in Materials and Methods and were examined for cell shape and nucleoid morphology by the fluo-phase technique (18). Shown is a composite of photographs at various time points after release from synchronization, in which the technically best photograph, as judged by visualization of cell morphology and nucleoid structure, was utilized. All photographs were from time points that were within 3 h after release from synchronization, and the comparison of an individual strain at the two temperatures (32 and 42°C) was done at the same time point within 30 min. (A) W3110 was used as a control and shows the expected rod shape of the cell with discrete nucleoids at both 32 and 42°C. (B) At the restrictive temperature of 42°C, strains harboring *dnaG2903* reveal clear filamentation and diffuse nucleoid staining. (C) The suppressor mutant, *sdgA5*, displays wild-type cell shapes and nucleoid patterns at both 32 and 42°C. Note that there is presumably only a single base pair difference between these three isogenic strains, yet there is a dramatic phenotypic difference at the nonpermissive 42°C.

membrane, and thus, this reagent may be separating DNA replication from membrane interaction domains (40, 45).

Combination fluorescence-phase-contrast microscopy reveals that *sdgA5* and *sdgA6* mutant strains clearly suppress both the aberrant cellular and nucleoid phenotypes of *dnaG2903*. Overexpression of the mutant protein, the *dnaG2903* product, in the *sdg* mutants compensates for these defects. Two possible models to explain suppression by overexpression of a mutant primase are as follows. (i) This domain provides structural rather than enzymatic function (i.e., interaction with another protein or membrane structure) where the total amount of a specific allele product is critical, or (ii) this mutant protein is unstable at 42°C. Evidence against the latter hypothesis is that *dnaP* (*dnaG2903*) mutant strains resume DNA synthesis rapidly after transfer to the permissive temperature, even in the presence of chloramphenicol (48). The fact that cell division is not restored even in the absence of chloramphenicol suggests that this mutation affects a function of primase that is distinct from its role in DNA synthesis (48). In support of the first model, quantitative compensation by overexpression of the mutant *dnaG2903* allele restores normal cell growth (21) (Fig. 1) and normal cell and nucleoid morphology (Fig. 6). In contrast, *dnaG3*, *dnaG308*, and *dnaG399* may affect more critical catalytic domains which cannot be ameliorated by overexpression.

Interestingly, the *E. coli dnaG399* allele could be complemented by a *dnaG*$^+$ gene from *S. typhimurium*, whereas the *dnaP* (*dnaG2903*) allele could not (34). The *dnaP* allele is more pleiotropic on DNA replication and cell division, as reflected by the differential reversibility of these effects. Complementation of the cell division defect of *dnaP* would not be detected in the assay utilized if a long phenotypic lag were required for phenotypic expression (34).

E. coli strains with *par* mutations display an abnormal nucleoid morphology phenotype which is presumably due to chromosome replication without partitioning and results in large nucleoids in the midcell. Chromosome partitioning involves decatenation of replicated chromosomes (topological resolution) as well as segregation of daughter chromosomes (topographical segregation) (22). The *parA* and *parD* alleles have been demonstrated to be mutations in the *gyrB* (23) and *gyrA* (20) genes, respectively. Recently, a new topoisomerase essential to chromosome partitioning, topoisomerase IV, has been identified and its two subunits have been defined by the mutations *parC* and *parE* (22). The *parC* gene demonstrates homology to *gyrA*, while *parE* demonstrates homology with *gyrB* (22). To date, *parB* is the only mutation which displays a chromosome-partitioning defect that is not in a topoisomerase gene. The phenotypes associated with *parB* and *dnaG2903* may reflect a role of DnaG in the topographical segregation of daughter chromosomes.

We propose a model in which chromosome partitioning depends on the attachment of the replisome to the membrane structure. In this model, DnaG is part of the replisome and its carboxy tail is part of a domain that links the replisome to other parts of the segregation machinery.

ACKNOWLEDGMENTS

We are grateful to the individuals named in Table 1 who provided bacterial strains. We thank Doug Berg, Carol Gross, Hiroshi Hiasa, Tsutomo Katayama, Yoshikazu Nakamura, and Malcolm Winkler for critical reviews of the manuscript and Linda Haway for preparation of the manuscript.

M. Grompe is an NICHHD fellow of the Pediatric Scientist Training Program, grant HD-22297. J. Versalovic is supported by the National Institutes of Health Medical Scientist in Training Program at Baylor College of Medicine. This research was supported by USPHS grant RR-05425, an Advanced Technology Program Grant from the Texas Higher Education Department, and an Abbott Laboratories Young Investigator of the Year Award (1989) to J.R.L. J.R.L. acknowledges support from the PEW Scholars Program in Biomedical Sciences.

REFERENCES

1. **Almond, N., V. Yajnik, P. Svec, and G. N. Godson.** 1989. An *Escherichia coli cis*-acting antiterminator sequence: the *dnaG nut* site. Mol. Gen. Genet. **216**:195–203.
2. **Bonhoeffer, F., and H. Schaller.** 1965. A method for selective enrichment of mutants based on high UV sensitivity of DNA containing 5-bromouracil. Biochem. Biophys. Res. Commun. **20**:93–97.
3. **Bouche, J. P., L. Rowen, and A. Kornberg.** 1978. The RNA primer synthesized by primase to initiate phage G4 DNA replication. J. Biol. Chem. **253**:765–769.
4. **Bouche, J. P., K. Zechel, and A. Kornberg.** 1975. *dnaG* gene product, a rifampicin-resistant RNA polymerase, initiates the conversion of a single strand coliphage DNA to its duplex replicative form. J. Biol. Chem. **250**:5995–6001.
5. **Boyer, H. W., and D. Roulland-Dussoix.** 1969. A complementation analysis of the restriction and modification of DNA in *Escherichia coli*. J. Mol. Biol. **41**:459–472.
6. **Burton, Z. F., C. A. Gross, K. K. Watanabe, and R. R. Burgess.** 1983. The operon that encodes the sigma subunit of RNA polymerase also encodes ribosomal protein S21 and DNA primase in *E. coli* K-12. Cell **32**:335–349.
7. **Carl, P. L.** 1970. *Escherichia coli* mutants with temperature-sensitive synthesis of DNA. Mol. Gen. Genet. **109**:107–122.
8. **Cotton, R. G. H.** 1989. Detection of single base changes in nucleic acids. Biochem. J. **263**:1–10.
9. **Cotton, R. G. H., and R. D. Campbell.** 1989. Chemical reactivity of matched cytosine and thymine bases near mismatched and unmatched bases in a heteroduplex between DNA strands with multiple differences. Nucleic Acids Res. **17**:4223–4233.
10. **Cotton, R. G. H., N. R. Rodrigues, and R. D. Campbell.** 1988. Reactivity of cytosine and thymine in single-base-pair mismatches with hydroxylamine and osmium tetroxide and its application to the study of mutations. Proc. Natl. Acad. Sci. USA **85**:4397–4401.
11. **Dahl, H. H., S. R. Lamande, R. G. Cotton, and J. F. Bateman.** 1989. Detection and localization of base changes in RNA using a chemical cleavage method. Anal. Biochem. **183**:263–268.
12. **Erickson, B. D., Z. F. Burton, K. K. Watanabe, and R. R. Burgess.** 1985. Nucleotide sequence of the *rpsU-dnaG-rpoD* operon from *Salmonella typhimurium* and a comparison of this sequence with the homologous operon of *Escherichia coli*. Gene **40**:67–78.
13. **Grompe, M., D. M. Muzny, and C. T. Caskey.** 1989. Scanning detection of mutations in human ornithine transcarbamoylase by chemical mismatch cleavage. Proc. Natl. Acad. Sci. USA **86**:5888–5892.
14. **Gross, J. D.** 1972. DNA replication in bacteria. Curr. Top. Microbiol. Immunol. **57**:39–74.
15. **Hiasa, H., H. Sakai, T. Komano, and G. N. Godson.** 1990. Structural features of the priming signal recognized by primase: mutational analysis of the phage G4 origin of complementary DNA strand synthesis. Nucleic Acids Res. **18**:4825–4831.
16. **Hiasa, H., H. Sakai, K. Tanaka, Y. Honda, T. Komano, and G. N. Godson.** 1989. Mutational analysis of the primer RNA template region in the replication origin ori_c of bacteriophage G4: priming signal recognition by *Escherichia coli* primase. Gene **84**:9–16.
17. **Hiasa, H., K. Tanaka, H. Sakai, K. Yoshida, Y. Honda, T. Komano, and G. N. Godson.** 1989. Distinct functional contributions of three potential secondary structures in the phage G4 origin of complementary DNA strand synthesis. Gene **84**:17–22.
18. **Hiraga, S., H. Niki, T. Ogura, C. Ichinose, H. Mori, B. Ezaki, and E. Jaffé.** 1989. Chromosome partitioning in *Escherichia coli*:

novel mutants producing anucleate cells. J. Bacteriol. **171**:1496–1505.
19. **Hirota, Y., J. Mordoh, and F. Jacob.** 1970. On the process of cellular division in *Escherichia coli*. III. Thermosensitive mutants of *E. coli* altered in the process of DNA initiation. J. Mol. Biol. **53**:369–387.
20. **Hussain, K., E. J. Elliott, and G. P. C. Salmond.** 1987. The ParD$^-$ mutant of *Escherichia coli* also carries a *gyrA* mutation. The complete sequence of *gyrA*. Mol. Microbiol. **1**:259–273.
21. **Katayama, T., Y. Murakami, C. Wada, H. Ohmori, T. Yura, and T. Nagata.** 1989. Genetic suppression of a *dnaG* mutation in *Escherichia coli*. J. Bacteriol. **171**:1485–1491.
22. **Kato, J., Y. Nishimura, R. Imamura, H. Niki, S. Hiraga, and H. Suzuki.** 1990. New topoisomerase essential for chromosome segregation in *E. coli*. Cell **63**:393–404.
23. **Kato, J., Y. Nishimura, and H. Suzuki.** 1989. *Escherichia coli parA* is an allele of the *gyrB* gene. Mol. Gen. Genet. **217**:178–181.
24. **Kogan, S. C., M. Doherty, and J. Gitschier.** 1987. An improved method for prenatal diagnosis of genetic diseases by analysis of amplified DNA sequences. Application to hemophilia A. N. Engl. J. Med. **317**:985–990.
25. **Lark, K. G.** 1972. Genetic control over the initiation of the synthesis of the short deoxynucleotide chains in *E. coli*. Nature (London) New Biol. **240**:237–240.
26. **Liebke, H., C. Gross, W. Walter, and R. Burgess.** 1980. A new mutation *rpoD*800, affecting the sigma subunit of *E. coli* RNA polymerase is allelic to two other sigma mutants. Mol. Gen. Genet. **177**:277–282.
27. **Lupski, J. R., and G. N. Godson.** 1984. The *rpsU-dnaG-rpoD* macromolecular synthesis operon of *E. coli*. Cell **39**:251–252.
28. **Lupski, J. R., and G. N. Godson.** 1989. DNA → DNA, and DNA → RNA → protein: orchestration by a single complex operon. Bioessays **10**:152–157.
29. **Lupski, J. R., A. A. Ruiz, and G. N. Godson.** 1984. Promotion, termination and anti-termination in the *rpsU-dnaG-rpoD* macromolecular synthesis operon of *E. coli* K-12. Mol. Gen. Genet. **195**:391–401.
30. **Lupski, J. R., B. L. Smiley, F. R. Blattner, and G. N. Godson.** 1982. Cloning and characterization of the *Escherichia coli* chromosomal region surrounding the *dnaG* gene, with a correlated physical and genetic map of *dnaG* generated via transposon Tn*5* mutagenesis. Mol. Gen. Genet. **185**:120–128.
31. **Lupski, J. R., B. L. Smiley, and G. N. Godson.** 1983. Regulation of the *rpsU-dnaG-rpoD* macromolecular synthesis operon and the initiation of DNA replication in *Escherichia coli* K-12. Mol. Gen. Genet. **189**:48–57.
32. **Maniatis, T., E. F. Fritsch, and J. Sambrook.** 1982. Molecular cloning: a laboratory manual. Cold Spring Harbor Laboratory, Cold Spring Harbor, N.Y.
33. **Marinus, M. G., and E. A. Adelberg.** 1970. Vegetative replication and transfer replication of deoxyribonucleic acid in temperature-sensitive mutants of *Escherichia coli* K-12. J. Bacteriol. **104**:1266–1272.
34. **Maurer, R., B. C. Osmond, E. Shekhtman, A. Wong, and D. Botstein.** 1984. Functional interchangeability of DNA replication genes in *Salmonella typhimurium* and *Escherichia coli* demonstrated by a general complementation procedure. Genetics **108**:1–23.
35. **Mead, D. A., E. Szczesna-Skorupa, and B. Kemper.** 1986. Single-stranded DNA 'blue' T7 promoter plasmids: a versatile tandem promoter system for cloning and protein engineering. Protein Eng. **1**:67–76.
36. **Murakami, Y., T. Nagata, W. Schwarz, C. Wada, and T. Yura.** 1985. Novel *dnaG* mutation in a *dnaP* mutant of *Escherichia coli*. J. Bacteriol. **162**:830–832.
37. **Nakamura, Y.** 1984. Amber *dnaG* mutation exerting a polar effect on the synthesis of RNA polymerase sigma factor in *Escherichia coli*. Mol. Gen. Genet. **196**:179–182.
38. **Nesin, M. J., J. R. Lupski, and G. N. Godson.** 1988. Role of 5′ upstream sequences and tandem promoters in regulation of the *rpsU-dnaG-rpoD* macromolecular synthesis operon. J. Bacteriol. **170**:5759–5764.
39. **Norris, V., T. Alliotte, A. Jaffé, and R. D'Ari.** 1986. DNA replication termination in *Escherichia coli parB* (a *dnaG* allele), *parA*, and *gyrB* mutants affected in DNA distribution. J. Bacteriol. **168**:494–504.
40. **Nunn, W. D., and B. E. Tropp.** 1972. Effects of phenethyl alcohol on phospholipid metabolism in *Escherichia coli*. J. Bacteriol. **109**:162–168.
41. **Paabo, S., and A. C. Wilson.** 1988. Polymerase chain reaction reveals cloning artifacts. Nature (London) **334**:387–388.
42. **Rowen, L., and A. Kornberg.** 1978. Primase, the *dnaG* protein of *Escherichia coli*: an enzyme which starts DNA chains. J. Biol. Chem. **253**:758–764.
43. **Rowen, L., and A. Kornberg.** 1978. A ribo-deoxyribonucleotide primer synthesized by primase. J. Biol. Chem. **253**:770–774.
44. **Sanger, F., S. Nicklen, and A. R. Coulson.** 1977. DNA sequencing with chain-terminating inhibitors. Proc. Natl. Acad. Sci. USA **74**:5463–5467.
45. **Silver, S., and L. Wendt.** 1967. Mechanism of action of phenethyl alcohol: breakdown of the cellular permeability barrier. J. Bacteriol. **93**:560–566.
46. **Smiley, B. L., J. R. Lupski, P. S. Svec, R. McMacken, and G. N. Godson.** 1982. Sequences of the *Escherichia coli dnaG* primase gene and regulation of its expression. Proc. Natl. Acad. Sci. USA **79**:4550–4554.
47. **van der Ende, A., T. A. Baker, T. Ogawa, and A. Kornberg.** 1985. Initiation of enzymatic replication at the origin of the *Escherichia coli* chromosome: primase as the sole priming enzyme. Proc. Natl. Acad. Sci. USA **82**:3954–3958.
48. **Wada, C., and T. Yura.** 1974. Phenethyl alcohol resistance in *Escherichia coli*. III. A temperature-sensitive mutation (*dnaP*) affecting DNA replication. Genetics **77**:199–220.
49. **Wang, L. F., and R. H. Doi.** 1986. Nucleotide sequence and organization of *Bacillus subtilis* RNA polymerase major sigma (sigma^{43}) operon. Nucleic Acids Res. **14**:4293–4306.
50. **Wechsler, J. A., and J. D. Gross.** 1971. *Escherichia coli* mutants temperature-sensitive for DNA synthesis. Mol. Gen. Genet. **113**:273–284.
51. **Wold, M. S., and R. McMacken.** 1982. Regulation of expression of the *Escherichia coli dnaG* gene and amplification of the *dnaG* primase. Proc. Natl. Acad. Sci. USA **79**:4907–4911.